Available online at www.sciencedirect.com
ScienceDirect
Journal of Power Sources 165 (2007) 757–763
JOURNAL OF POWER SOURCES
www.elsevier.com/locate/jpowsour

Fabrication, microstructure and properties of a YSZ electrolyte for SOFCs

Minfang Han *, Xiuling Tang, Huiyan Yin, Suping Peng

Union Research Center of Fuel Cell, School of Chemical & Environment Engineering, China University of Mining & Technology (CUMTB), Beijing 100083, China

Received 24 July 2006; received in revised form 6 November 2006; accepted 17 November 2006
Available online 30 January 2007

Abstract

Yttria stabilized zirconia (YSZ) has widely been used as an electrolyte in solid oxide fuel cell (SOFC) stacks. The microstructure and properties of YSZ related to the fabrication process are discussed in this paper. For the named two-step sintering process, uniform and hexagonal grains with a size of 1–4 μm were obtained from the adobe following tape calendaring (TCL). Elliptical and hexagonal grains with a size of 0.4–3 μm were obtained from the adobe of tape casting (TCS) using the three-step process. The electrical conductivities of YSZ with different grain sizes were measured via the four-probe DC technique and grain conductivities and grain boundary conductivities of YSZ were investigated by impedance spectroscopy. YSZ electrolytes with a grain size of 0.1–0.4 μm had the highest electrical conductivity in the range of 500–1000 °C, especially at medium and low temperatures 550–800 °C. As the YSZ grain size becomes small, the thickness of the intergranular region decreased greatly. The YSZ electrolytes with sub-micrometer grain sizes, high ion conductivity and low sintering temperatures are important to the electrode-supported SOFC, on which the dense YSZ electrolyte films are optimized at 10 μm.

Keywords: SOFC; Yttria stabilized zirconia (YSZ); Electrolyte; Sub-micrometer grain

1. Preface

Solid oxide fuel cells (SOFCs) are the most efficient devices yet invented for conversion of chemical fuels directly into electrical power. The high operating temperature (600–1000 °C) of SOFCs has a number of advantages, such as all solid state components, the feasibility of running the cells directly on practical hydrocarbon fuels without an external fuel reformer that is necessary for low-temperature fuel cells, high temperature heat to drive a gas turbine and lower emissions. The solid state electrolyte used in SOFCs are required for high ionic conductivity, better stability, chemical and thermal compatibility, impermeability by the reacting gases, high strength and toughness, easy fabrication and low cost [1]. As the key component of SOFCs, the solid electrolyte materials mainly include fluorite-structured stabilized zirconia [2], doped ceria [3] and perovskite-structured $LaGaO_3$ [4]. Yttria stabilised zirconia (YSZ) is now still mostly used in the SOFC stack. In anode-supported cells, a YSZ and Ni-YSZ cermet are required to co-fire [5] during 1350–1400 °C [6]. In cathode-supported cells, YSZ and doped lanthanum manganite (LSM) ceramic are required to co-fire during 1200–1250 °C [7,8]. Therefore, it is very important to reduce the sintering temperature of the YSZ. In electrode-supported cells, it is necessary to decrease the thickness of the dense electrolyte film in order to reduce the ohmic polarization. The thickness of the YSZ film is about 10 μm [9], thus fine YSZ grains are necessary for thin electrolyte densification and performance. However, due to the high surface energy among the cubic YSZ grains, they grow easily during the sintering process [10]. Therefore, it is necessary to research the growth and stabilization of the YSZ grains, which are dense and fine, at lower temperature.

2. Experiment

YSZ nano-powders are usually used as the raw materials, which are made by a liquid-phase method [11]. The diameter of the grains by TEM is 10–15 nm [12], and the distribution of the powder is narrow, approximately 0.1–0.3 μm [12]. The powders

* Corresponding author. Tel.: +86 10 62341427; fax: +86 10 62331098.
E-mail address: hmf121@hotmail.com (M. Han).

0378-7753/$ – see front matter © 2006 Elsevier B.V. All rights reserved.
doi:10.1016/j.jpowsour.2006.11.054

are uniform and spherical and there are no hard agglomerates among them [13]. With the above powders, the film adobes of YSZ were made by tape casting (TCS) [14,15], tape calendaring (TCL) [16] and a gel casting (GC) process [17]. The samples were cut to discs with a diameter 20 mm and a thickness of 0.2–0.3 mm.

The YSZ electrolytes were sintered in a high temperature box furnace (type-GXL-34/30/40). The density was measured by the Archimedes method. The grain size and microstructure were observed by SEM (GSM6700, Japanese). The electrical conductivity of the YSZ electrolytes, which were sintered by different processes, was measured via four-probe DC technique. The AC impedance analyzer (Agilent 4294A) was used for the AC impedance measurement over the frequency range of 40 Hz to 110 MHz.

3. Results and discussion

3.1. Sintering process, crystal grain size and microstructure of YSZ

The sintering properties of YSZs powders [18–20] are such that the YSZ powder begins to be sintered at 800–1000 °C, which is relative to the grain diameter, i.e. the smaller the grain size, the lower the start of sintering. The most rapid sintering rate of the YSZ occurs at 1150–1280 °C, and the sintering process is complete at 1400–1450 °C [18–20]. According to the sintering properties of YSZ powder [18–20], three kinds of methods were used to sinter the YSZ ceramic materials in the range of 1250–1550 °C, including an one-step sintering process, a two-step sintering process and a three-step sintering process.

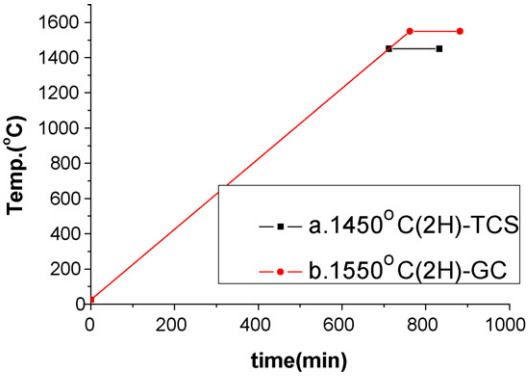

Fig. 1. Temperature to time in one-step sintering process.

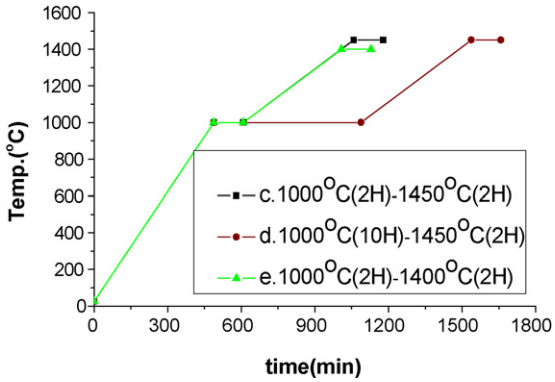

Fig. 3. Temperature to time in two-step sintering process.

The one-step sintering process was carried out in the range of 1450–1550 °C, as shown in Fig. 1. The heating rate from R.T. to sintering temperature is 2 °C min^{-1} and then fired for different times, about 2–6 h. This is the traditional sintering process of a ceramic [21]. The microstructure of YSZs is shown in Fig. 2. The uniform and clear grains with a size of 3–5 μm were obtained from the adobe of tape casting by sintering at 1450 °C for 2 h. Pores are seldom found in the grain boundaries. The grain size from the gel casting process sintering at 1550 °C for 2 h is 8–15 μm, with a clear boundary during the grains. Because of the higher sintering temperature, over-sintering appeared. As a result, the most suitable process for one-step sintering is 1450 °C for 2–4 h.

The two-step sintering process was carried out in the range of 1400–1450 °C, as shown in Fig. 3. The adobe was firstly sintered at 1000 °C for 2–10 h, then raised to 1400–1450 °C at the rate of 1 °C min^{-1}, finally it was fired for 2 h. The microstructure of YSZs is shown in Fig. 4. The uniform and clear grains with a size of 1–4 μm were obtained from the adobe of tape calendaring. As a result, the suitable process for two-step sintering was 1000 °C for 2 h, (1400–1450) °C for 2 h.

The three-step sintering process was carried out in the range of 1250–1300 °C, as shown in Fig. 5. The adobe was firstly sintered at 1000 °C for 2 h, then the temperature was raised at a rate of 0.8 °C min^{-1} to 1400 °C, then decreased

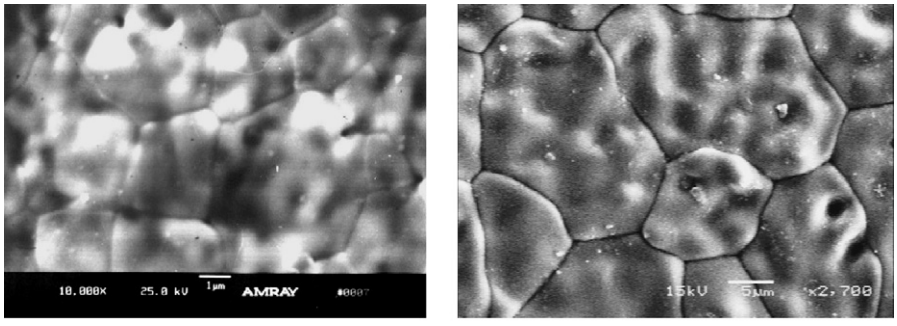

(a) **1450°C X 2H-TCS** (b) **1550°C X 2H-GC**

Fig. 2. Microstructure of YSZ made by one-step sintering process.

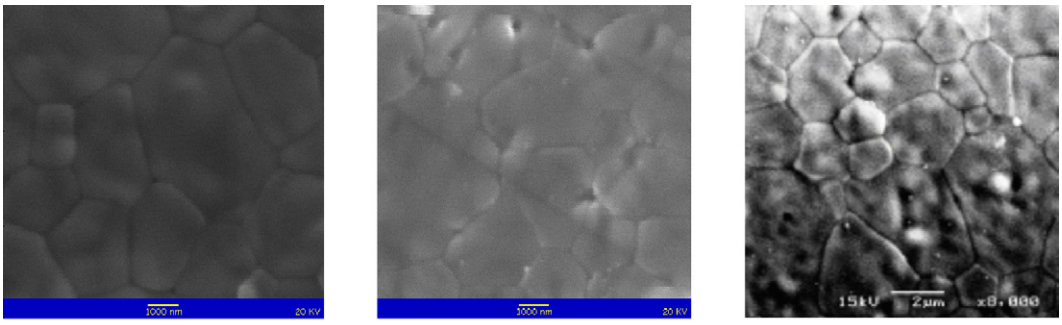

Fig. 4. Microstructure of YSZ (TCL) made by two-step sintering process.

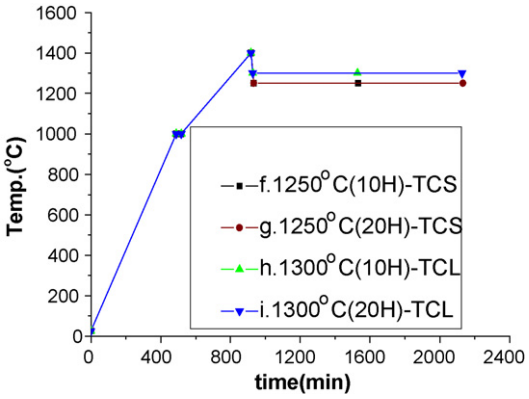

Fig. 5. Temperature to time in three-step sintering process.

directly to 1250–1300 °C in 30 min, the furnace was controlled at 1250–1300 °C for 10–20 h. The microstructure of YSZs is shown in Fig. 6. The uniform and clear grains with a size of 0.4–1 μm were obtained from the adobe of tape casting.

During the sintering processes of YSZ, there are two steps: the crystallization behavior at low temperature—about 800–1000 °C, and grain growth behavior at high temperature of more than 1100 °C [10].

The YSZ nuclei crystallize out from the amorphous precursors by surface diffusion, which overcome the barrier of surface energy. Assuming that the nuclei were spherical, the initial crystallite (nuclei) size d_c would be [10]:

$$d_c = \frac{3\gamma_s M}{4\rho\Delta G} \quad (1)$$

where ΔG is the Gibbs' energy increment for the phase transformation from the amorphous phase of the precursors to the crystalline phase, γ_s the surface energy, ρ the density of the crystallized phases and M is the molecular weight concerned.

During the YSZ sintering process, only those grains with the size of YSZ nuclei $d \geq d_c$ by surface diffusion, begin to grow in the later steps. If this period of YSZ nuclei crystallization was passed quickly, as in the one-step process of Fig. 1, then there would be only a few nuclei whose sizes are bigger than d_c, and thus a small quantity of stabilized grain would be kept growing. Due to the large space among the YSZ nuclei, the energy for the YSZ grain growth is high and the way for YSZ grain growth to touch the adjacent grain is long. So, the sintering temperature of YSZ with a larger size as shown in Fig. 2 is high. Holding a certain time (e.g. 2 h) in the range of 800–1000 °C, as in the two-step process of Fig. 2, would help to form a great deal of nuclei whose sizes are bigger than d_c. These nuclei keep growing by grain boundary motion. Because so many nuclei are formed, there is a short distance between each other. In the end, the grain size is smaller, and at the same time adense YSZ was obtained, as shown in Fig. 4c. Furthermore, the dense YSZ with fine grains was obtained at a lower sintering temperature of about 1400 °C as shown in Fig. 4e. However, if the process of nuclei formation is too long (e.g. 10 h), the formed nuclei will be inactive and will not benefit from grain growth at a later time. As a result, the YSZ grains would be grown incompletely. After the YSZ adobes were held for 10 h in 1000 °C and sintering 1450 °C for 2 h, the YSZ grains are not perfect. There are many intergranular pores in the YSZ grain boundaries, as shown in Fig. 4d.

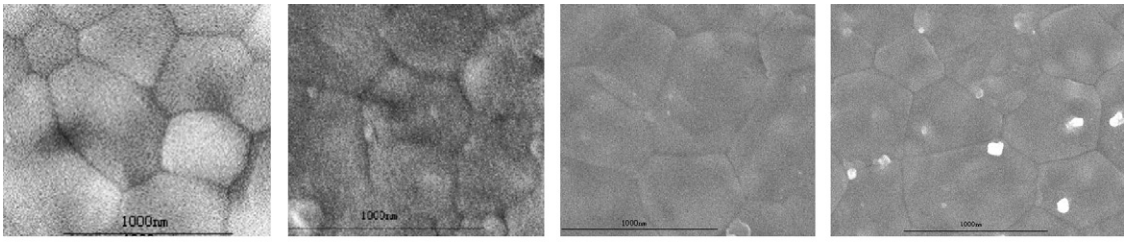

Fig. 6. Microstructure of YSZ (TCS) made by three-step sintering process.

The grain growth is a result of grain boundary motion, which contains two processes: grain boundary diffusion and grain boundary migration. At relatively low temperatures, according to Harmer and Brook [22], grain boundary diffusion may proceed; then at elevated temperatures, grain boundary migration becomes a dominant mechanism for grain growth. It is suggested that grain boundary migration may involve an activation process that needs a higher activation energy than grain boundary diffusion. The feasibility of densification without grain growth relies on the suppression of grain boundary migration while keeping grain boundary diffusion active [23], so the dense and fine YSZ of the three-step sintering method as shown in Fig. 5 was obtained. When the adobe was sintering up to 1400 °C, there is enough energy both for grain boundary diffusion and for grain boundary migration. Then the temperature is decreased to 1250–1300 °C, which can suppress grain boundary migration but not affect grain boundary diffusion, and as a result, the YSZ grain size stays within a certain range, of less then 1 μm. In this way, the YSZ grain does not increase dramatically as in the conventional sintering method, and dense ceramic bodies were achieved. The rate of grain boundary diffusion is much lower than that of grain boundary migration. In order to ensure the sufficiency of grain boundary diffusion, a relatively long time such as 10–20 h are needed at 1250–1300 °C. At last, the dense YSZs with finer grains ~0.1–1 μm were obtained, as shown in Fig. 6.

3.2. YSZ Electrical conductivity related to grain size

There are four different grain sizes in YSZ electrolytes, which are 0.1–0.4, 0.3–1.5, 1–5 and 8–15 μm, respectively, by different sintering processes. The conductivities of YSZ with various sizes are shown in Fig. 7. As a result, all of them could be used as the electrolyte in SOFC. At higher temperature periods, e.g. 850–1000 °C, there are no obvious differences in conductivity among the four-different grain sizes. But, at medium and lower temperatures, e.g. 550–800 °C, the YSZ electrolytes with a smaller grain size, such as 0.1–0.4 and 0.3–1.5 μm, obviously have higher conductivities than others with a larger grain size, such as 1–5 and 8–15 μm. With a temperature decrease in the range of 550–800 °C, the difference of electrical conductivities of YSZ electrolytes increases.

For dense ceramic solid electrolytes, the effect of pores is minor and can be ignored. The conductivity of the solid electrolyte is made up of grain conductivity and grain boundary conductivity. In the light of traditional solid-state ionic conductive theory, grain conductivity is higher by two or three times than in the grain boundary [24]. The properties of the intergranular region play an important role in the overall conductivity of the electrolyte. Poor conductivity of the electrolyte is usually due to low conductivity of the intergranular region. Sometimes, the conductivity of the grain interior is typically higher by two or three times than that of the grain boundary [24]. Many factors, such as grain size, intergranular area, impurity level and intergranular thickness, significantly affect the apparent intergranular conductivity. It is suggested that there are two main reasons for low grain-boundary conductivity. Firstly, there is a space-charge layer near the grain boundary formed by solute segregation or a blocking layer for oxygen conduction formed by impurity phases. The other is that the conduction of oxygen ions decreases when the oxygen-vacancy concentration at the grain boundary becomes lower than that in the grain interior [25]. Especially at low temperature, the impurity at the grain boundary has more of an effect on the total ion conductivity.

In a YSZ electrolyte, as the YSZ grain size becomes smaller and smaller, the thickness of the intergranular region decreases greatly, as shown in Fig. 8. There are only 1–3 atom layers in the intergranular region, which is totally different from the above discussion [26]. There is hardly any solute segregation or impurity phase in the region to form a blocking layer for oxygen ion conduction. As we assumed, the oxygen-vacancy concentration at the grain boundary for oxygen ion conduction

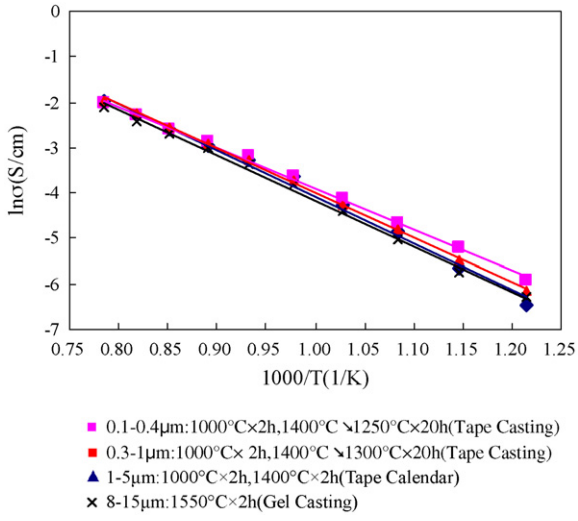

Fig. 7. The conductivities of YSZ with different grain sizes.

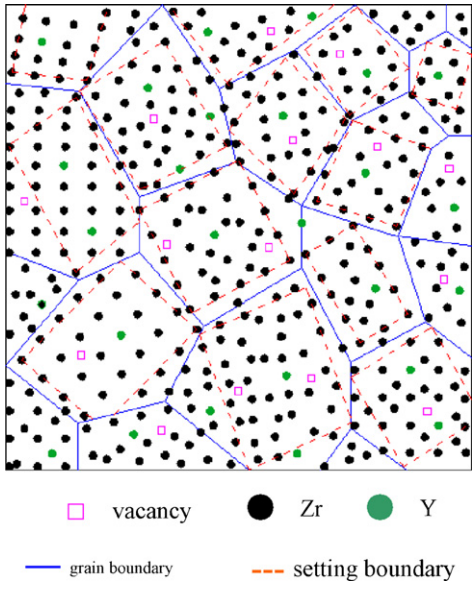

Fig. 8. Microstructure models of sub-micrometer YSZ crystalline samples.

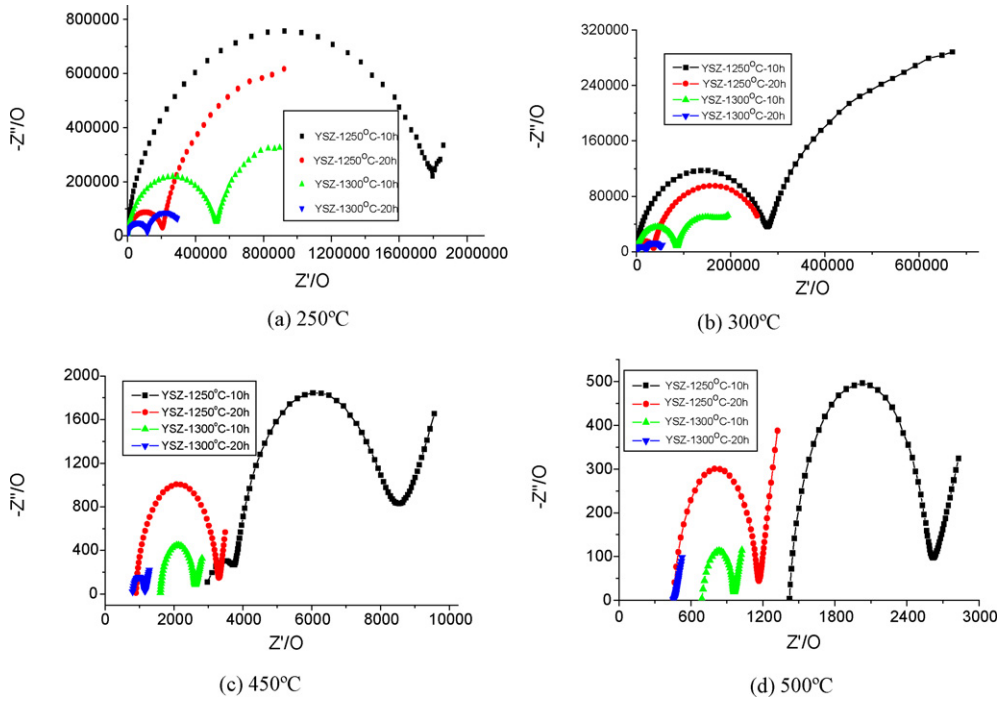

Fig. 9. Impedance spectroscopy of YSZs at different temperature.

is not lower, but higher. So the intergranular conductivity would increase.

In order to correlate the microstructure of the electrolyte with the intergranular conductivity, a improved simple model [27], such as 'brick layer model', can be used to comprehend the electrical properties of the intergranular region using Eq. (2):

$$\sigma_{\text{app, gb}} = \frac{\sigma_{\text{sp, gb}} d_{\text{g}} A}{\delta_{\text{gb}} S} \tag{2}$$

where $\sigma_{\text{app, gb}}$ is the apparent intergranular conductivity based on the electrolyte geometrical dimension, $\sigma_{\text{sp, gb}}$ the specific intergranular conductivity, d_{g} the grain size of the electrolyte, δ_{gb} the thickness of the intergranular, A the total effective conducting area, which is related to the intergranular area and S is the electrode area.

With the decreasing of grain size d_{g}, the thickness of the intergranular δ_{gb} decreased and the specific intergranular conductivity $\sigma_{\text{sp, gb}}$ increased. With the decreasing of grain size d_{g}, intergranular area increased, thus that the total effective conducting area A increased. It is obvious that the decreasing rate of grain size (reduced as the correlative grain size's first power) is largely lower than the increasing rate of total effective conductive area (increased as the correlative grain size's quadratic). So the total conductivity of YSZ with sub-micrometer grain size would increase largely. For microcrystalline samples, the conductivities of the bulk and the grain boundary are in the same range [28]. Furthermore, due to the much smaller grain size, the specific grain boundary conductivity of the nanocrystalline samples is 1 and 2 orders of the magnitude higher than that of the microcrystalline samples [28]. As a consequence, the total ionic conductivities of the nanocrystalline samples are enhanced.

3.3. Impedance spectroscopy analysis

The YSZ electrolytes with different sintering processes were measured by impedance analyzer (Agilent 4294A), as shown in Fig. 9. During the three-step sintering process, the sintering temperature is in the range of 1250–1300 °C. With the sintering temperature increasing and the holding time lengthening, the intergranular resistance is obviously reduced, and intragranular resistance is also relatively reduced. Fig. 10 shows that the relative densities of YSZ with different processes are about 96–99%, and increase with the sintering temperature increasing and the holding time lengthening.

It is reasonable to assume that the pores are well distributed within the electrolyte and the intergranular region. Thus, the relative density can be simply calculated by Eq. (3) [26]:

$$\xi = \frac{V_{\text{r}}}{V_{\text{g}}} = \frac{S_{\text{r}} L}{S_{\text{g}} L} = \frac{S_{\text{r}}}{S_{\text{g}}} \tag{3}$$

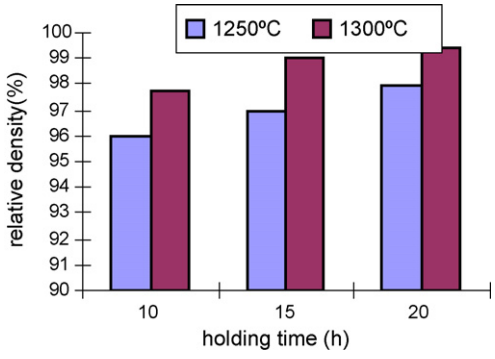

Fig. 10. YSZ relative density related to holding time at different sintering temperature.

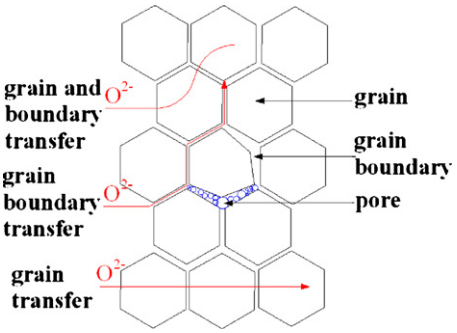

Fig. 11. Schematic diagram of oxygen ions transportation.

where ξ is the relative density, S_r and V_r are real surface area and real volume occupied by the solid, S_g, V_g and L are geometric surface area, geometric volume and thickness of the electrolyte, respectively.

According to the schematic diagram Fig. 11 and Ohmic law, the resistance of oxygen ion transportation through the grains could be expressed as follows:

$$R_g = \frac{L\tau}{\sigma_{sp,\,gi} S_r} = \frac{L}{\sigma_{app,\,si} S_g} \quad (4)$$

where R_g is the electrical resistance of grains, τ the torturous factor which is used to correct the real transportation path through the grains, $\sigma_{app,\,gi}$ and $\sigma_{sp,\,gi}$ are the apparent intragranular conductivity based on the geometric dimension and specific intragranular conductivity.

Substituting Eqs. (3) and (4), the apparent intragranular conductivity as a function of microstructure can be obtained.

$$\sigma_{app,\,gi} = \frac{\sigma_{sp,\,gi}\xi}{\tau} \quad (5)$$

Eq. (5) not only gives satisfactory explanation to the linear relationship between the apparent intragranular conductivity and the relative density but also highlights the slight difference of the intragranular resistance between the electrolytes with close relative density and different grain size. This difference may be due to the different value of the torturous factor τ, which is related to the microstructure of the electrolyte.

As to the intergranular conductivity, it is seriously affected by the microstructure of the intergranular region. In the three-step sintering process, the pores gradually disappeared from the intergranular region by grain boundary diffusion. With the sintering temperature increasing (from 1250 to 1300 °C) and the holding time extending (from 10 to 20 h), grain boundary diffusion became more and more sufficient. The pores in the intergranular region become less and smaller, so that intergranular resistance decreased greatly, related to the result shown in Fig. 9.

4. Conclusion

YSZ solid electrolytes with different grain sizes in the range of 0.1–15 μm were obtained by controlling the sintering processes. Sub-micrometer grain sizes such as 0.1–1 μm in YSZs were obtained by a three-step sintering process, which was performed at 1000 °C for 2–10 h, then raising the temperature at the rate of 0.8 °C min^{-1} to 1400 °C, then by decreasing it directly to 1250–1300 °C in 30 min, the furnace was controlled at 1250–1300 °C for 10–20 h. YSZ electrolyte with a grain size of 0.1–0.4 μm had the highest conductivity in the range of 500–1000 °C, especially at medium and low temperatures 550–800 °C. As the YSZ grain size became small, the thickness of the intergranular region decreased greatly. There are only 1–3 atom layers in the intergranular region, where there is hardly the solute segregation or impurity phase in the region to form a blocking layer for oxygen ion conduction. YSZ electrolytes with sub-micrometer grain sizes, high ion conductivity and low sintering temperature are important to an electrode-supported SOFC, on which dense YSZ electrolyte films are optimized at 10 μm.

Acknowledgements

The projects were supported by Ministry of Education, China, under the grant number 106087 and 863 Program of National High Technology Research Development Project, China, under the grant number 2005AA501050.

References

[1] M. Han, S. Peng, Solid Oxide Fuel Cell Components and Manufacture Processes, Chinese Science Press, Beijing, 2004, p. 2 (in Chinese).
[2] N.Q. Minh, T. Takahashi, Science and Technology of Ceramic Fuel Cells, Elsevier, Amsterdam, 1995.
[3] B.C. Steele, in: T. Takahashi (Ed.), High Conductivity Solid Ionic Conductors, World Scientific, Singapore, 1989.
[4] J.W. Stevenson, K. Hasinska, N.L. Canfield, et al., J. Electrochem. Soc. 147 (9) (2000) 3213–3218.
[5] W. Bao, Q. Chang, G. Meng, J. Membrane Sci. 259 (2005) 103–109.
[6] R.N. Basu, G. Blass, J. Eur. Ceram. Soc. 25 (2005) 463–471.
[7] H. Orui, K. Watanabe, M. Arakara, J. Power Sources 112 (2002) 90–97.
[8] K. Yamahara, C.P. Jacobson, S.J. Visco, et al., Solid State Ionics 176 (2005) 451–456.
[9] S.C. Singhal, K. Kendall, High Temperature Solid Oxide Fuel Cells: Fundamentals, Design and Applications, Esevier Ltd., 2003, p. 103.
[10] J.L. Shi, M.L. Ruan, T.S. Yen, Ceram. Int. 22 (1996) 137–142.
[11] M. Han, S. Peng, Z. Sun, Q. Duan, Proceeding of U.S.-China Clean Energy Technology Forum, I, Beijing, China, August 2001, pp. 161–169.
[12] M. Han, B. Li, S. Peng, J. Univ. Yunan 24 (1) (2002) 29–32.
[13] H. Yin, M. Han, The Fourth China International Conference on High-Performance Ceramics, Chengdu, China, October 2005, pp. 211–212.
[14] M. Han, Y. Wang, B. Li, S. Peng, J. Univ. Sci. Technol. Beijing 27 (2) (2005) 209–212.
[15] M. Han, S. Peng, C. Yang, Y. Wang, B. Li, Funct. Mater. 34 (5) (2003) 540–542.
[16] M. Han, C. Yang, B. Li, S. Peng, Battery 34 (3) (2004) 207–208.
[17] M. Han, H. Yin, X. Tang, S. Peng, in: B. Zhu, Z. Mao (Eds.), Proceeding of the 4th Sino-Swedish Fuel Cell Workshop and Joint Energy-Environment Forum, Haerbin, China, October 2005, pp. 65–68, ISBN: 7283-796-9.
[18] M. Han, L. Huo, B. Li, S. Peng, J. Univ. Sci. Technol. Beijing 12 (1) (2005) 78–80.
[19] M. Han, B. Li, S. Peng, J. Wuhan Univ. Technol., Mater. Sci. 19 (3) (2004) 10–13.
[20] M. Han, S. Peng, B. Li, Rare Metal Mater. Eng. 32 (2003) 491–495.

[21] R.J. Brook (Ed.), Processing of Ceramics, Materials Science and Technology, vol. 17B, Press of Science, 1999, pp. 75–77.
[22] M.P. Harmer, R.J. Brook, J. Brit. Ceram. Soc. 80 (5) (1980) 147.
[23] I.-W. Chen, X.-H. Wang, Nature 404 (2000) 168–171.
[24] X.J. Chen, K.A. Khor, S.H. Chan, et al., Mater. Sci. Eng. A 374 (2004) 64–71.
[25] J.-H. Lee, T. Mori, J.-G. Li, et al., J. Electrochem. Soc. 147 (7) (2000) 2822–2829.
[26] Z. Guan, Z. ZHANG, J. Jiao, Physical Properties of Inorganic Materials, 3, Tsinghua University Press, 1992, p. 265.
[27] X.J. Chen, K.A. Khor, S.H. Chan, et al., Mater. Sci. Eng. A 335 (2002) 246–252.
[28] P. Mondal, A. Klein, W. Jaegermann, H. Hahn, Solid State Ionics 118 (1999) 331–339.